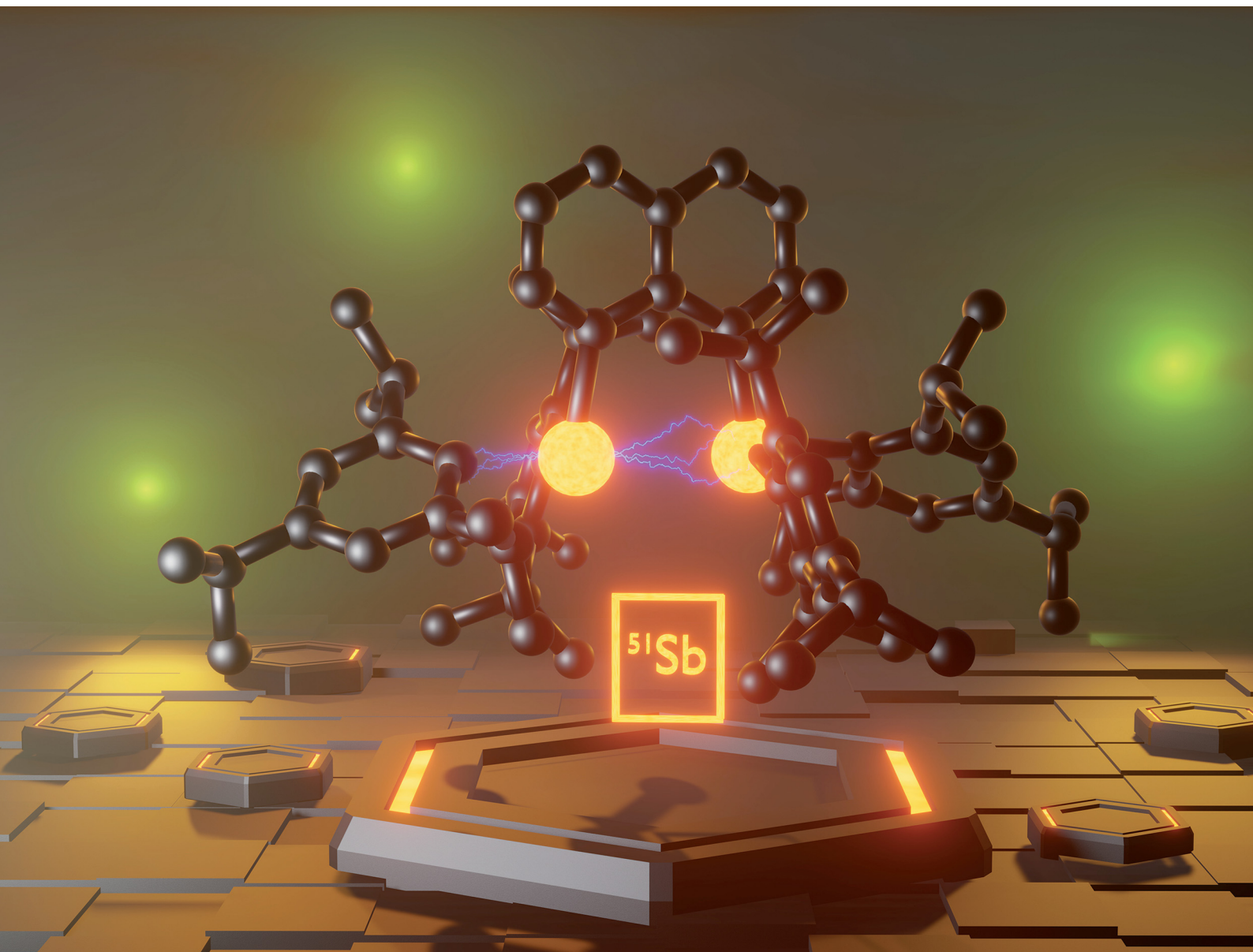


ChemComm

Chemical Communications

rsc.li/chemcomm



ISSN 1359-7345

COMMUNICATION

Gebhard Haberhauer, Stephan Schulz *et al.*
Bisstibane–distibane conversion *via* consecutive
single-electron oxidation and reduction reaction



Cite this: *Chem. Commun.*, 2022, 58, 6682

Received 7th April 2022,
Accepted 10th May 2022

DOI: 10.1039/d2cc01986h

rsc.li/chemcomm

Bisstibane–distibane conversion *via* consecutive single-electron oxidation and reduction reaction†

Alexander Gehlhaar,^a Hanns Micha Weinert,^b Christoph Wölper,^a Nina Semleit,^b Gebhard Haberhauer^b and Stephan Schulz^a*

peri-Substituted naphthalene complexes (Trip₂Pn)₂Naph (Pn = Sb 1, Bi 2) were synthesised and their redox behaviour investigated. Oxidation of 1 with [Fc][BAR^F] (BAR^F = B(C₆F₅)₄) yielded [(Trip₂Sb)(-TripSb)Naph][BAR^F] (3) containing the stibane-coordinated stibonium cation [(Trip₂Sb)(TripSb)Naph]⁺. Subsequent reduction of 3 with KC₈ yielded distibane (TripSb)₂Naph (4). 1–4 were characterised by NMR (¹H, ¹³C) and IR spectroscopy as well as single-crystal X-ray diffraction (sc-XRD), while their electronic structures were analysed by quantum chemical computations.

The utilisation of donor–acceptor bonding in chemical synthesis has received increasing interest since the development of frustrated Lewis acid–base pairs (FLPs) by Stephan *et al.* almost 15 years ago.¹ FLPs are ambiphilic species due to the presence of both a Lewis basic and a Lewis acidic center, which were used in bond activation reactions and organic transformations.² FLPs are mainly based on N/B, P/B, P/Al combinations, but related systems have also been reported,³ including P-coordinated tetrylenes⁴ and *peri*-substituted naphthalene complexes with P→E and EB (E = Sn, Pb) interactions.⁵ In contrast, comparable complexes containing heavy pnictogen atoms are rare.

Neutral donor–acceptor complexes R₃Pn–Pn′R′₃ of Lewis basic phosphanes PR₃ (R = alkyl, aryl) and Lewis acidic phosphanes PX₃ (X = halide)⁶ as well as their heavier homologues are well known.^{7–9} Since donor–acceptor interaction strengths typically decrease with increasing atomic number, neutral complexes of heavy pnictogens tend to dissociate to either the

neutral Lewis acid and Lewis base or with formation of ionic species [R₃Pn–Pn′R′₂]⁺[R′][−] (Fig. 1), which are often more stable toward Pn–Pn′ bond dissociation due to the increased Lewis acidity of the pnictenium (Pn′R′₂⁺) cation.^{8–11} *peri*-Substituted naphthalene and acenaphthene complexes, in which the pnictogen atoms are fixed in 1,8-position, are also promising candidates to study Pn(III)–Pn(III) donor–acceptor interactions since they can not separate into two individual species. While complexes of this type containing lighter pnictogens are known,¹² those of the heaviest elements of group 15, Sb and Bi, are still rare, and they exclusively contain rather strong phosphane donors.¹³

We recently reported on dipnictanes Pn₂Naph₂ (Pn = As, Sb, Bi)¹⁴ and bis(diphenylpnicta)naphthalenes (Ph₂Pn)₂Naph (Pn = Sb, Bi)¹⁵ of the heaviest group 15 elements. Due to our general interest in pnictogen-centered radicals,¹⁶ we investigated single electron transfer reactions of the latter. Unfortunately, reactions with several oxidants failed to give defined reaction products. We therefore replaced the Ph groups by bulky Trip groups (Trip = 2,4,6-*i*-Pr₃C₆H₂), which successfully stabilised Trip₃Pn^{•+} radical cations,¹⁷ in order to kinetically stabilise

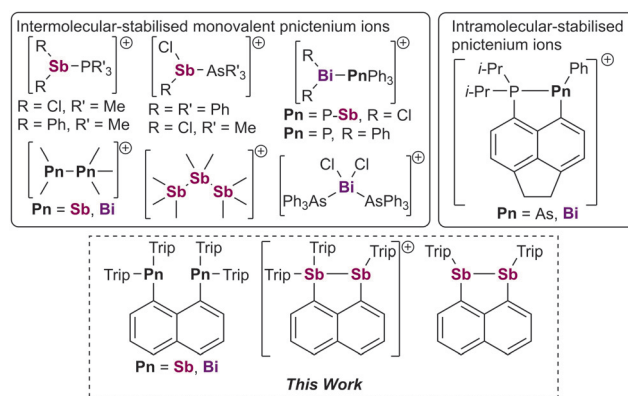


Fig. 1 Known intermolecular- and intramolecular stabilised pnictenium cations and *peri*-substituted heavy pnictenium complexes reported herein.

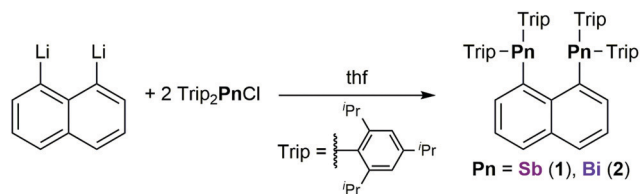
^a Institute of Inorganic Chemistry, University of Duisburg-Essen, 45117 Essen, Germany. E-mail: stephan.schulz@uni-due.de

^b Institute of Organic Chemistry, University of Duisburg-Essen, 45117 Essen, Germany. E-mail: gebhard.haberhauer@uni-due.de

^c Center for Nanointegration Duisburg-Essen (Cenide), University of Duisburg-Essen, Carl-Benz-Strasse 199, 47057 Duisburg, Germany

† Electronic supplementary information (ESI) available: Experimental procedures, NMR and IR spectra, elemental analysis, crystallographic data and details of theoretical study. CCDC 2157418 (1), 2157419 (2), 2157420 (3), and 2157421 (4). For ESI and crystallographic data in CIF or other electronic format see DOI: <https://doi.org/10.1039/d2cc01986h>





Scheme 1 Synthesis of sterically crowded bispnictanaphthalenes **1** and **2**.

likely-formed radical cations. (Trip₂Pn)₂Naph (Pn = Sb **1**, Bi **2**) were synthesized by reaction of Trip₂PnCl (Pn = Sb, Bi) with Li₂Naph at $-78\text{ }^{\circ}\text{C}$ (**1**) and $-30\text{ }^{\circ}\text{C}$ (**2**), respectively (Scheme 1).

The ¹H NMR spectrum of **2** at ambient temperature shows the expected number of signals due to the Naph and Trip substituents, indicating a symmetric molecule in solution, whereas that of **1** exhibits several signals of the Trip groups, pointing to a molecule of lower symmetry. Variable temperature (VT) NMR studies showed that the septet of the *ortho* i-Pr group first splits into two broad signals, which further split into two septets. ΔG^{\ddagger} values of 15.6 and 15.9 kcal mol⁻¹ were calculated from the coalescence temperatures ($50\text{ }^{\circ}\text{C}$, $70\text{ }^{\circ}\text{C}$).¹⁸ **2** also shows coalescence points ($0\text{ }^{\circ}\text{C}$, $\Delta G^{\ddagger} = 12.9\text{ kcal mol}^{-1}$; $-60\text{ }^{\circ}\text{C}$, $\Delta G^{\ddagger} = 13.3\text{ kcal mol}^{-1}$) at lower temperatures. The hindered rotation most likely stems from ligand–ligand interactions of the large Trip groups, which are expected to be larger in **1** due to the smaller Sb atoms compared to the Bi atoms in **2**, resulting in larger rotational barriers in **1**.

Single crystals of **1** (Fig. 2A) and **2** (Fig. S26, ESI[†]) were grown from saturated solutions in ethanol upon storage at $+4\text{ }^{\circ}\text{C}$. **1** and **2** crystallise in the orthorhombic and monoclinic space groups *P*2₁2₁2 (**1**) and *C*2/*c* (**2**) with two (**1**) and four (**2**) molecules per unit cell, respectively. Selected bond lengths and angles are given in Table 1.

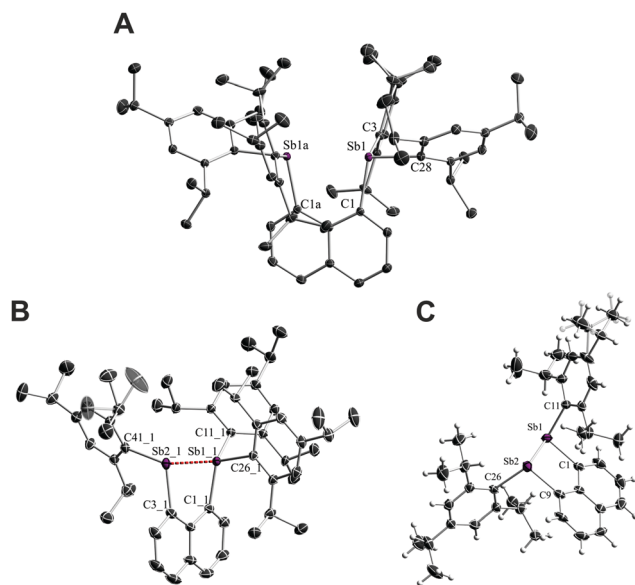


Fig. 2 Solid-state structures of **1** (A), **3** (B), and **4** (C) with displacement ellipsoids drawn at the 50% probability level. Hydrogen atoms (**1**, **3**) and the [BarF⁻] anion (**3**) are omitted for clarity.

The pnictogen atoms adopt trigonal-pyramidal coordination spheres, and the sum of bond angles (306.02° **1**, 296.56° **2**) indicate a high p-orbital character of the bonding electrons. The Sb–C (2.1769(11) Å, 2.2019(11) Å, 2.1902(10) Å) and Bi–C (2.318(4) Å, 2.326(5) Å, 2.326(5) Å) bonds are rather long due to the large steric crowding in **1** and **2**. Despite the increased steric hindrance, the Sb···Sb distance in **1** (3.2327(2) Å) is shorter than that in (Ph₂Sb)₂Naph (3.2983(6) Å),¹⁵ indicating stronger attractive forces, *i.e.* ligand···ligand dispersion interactions of the i-Pr groups of the Trip substituents. In marked contrast, the Bi···Bi distance in **2** (3.6742(4) Å) is significantly elongated compared to that in (Ph₂Bi)₂Naph (3.4461(4) Å).¹⁵ The elongation of the Pn···Pn distance in **2** compared to **1** points to stronger repulsive interactions between the Bi atoms, which is also reflected by the larger distortion of the Naph ligand in **2** (dihedral angles: $12.78(7)^{\circ}$ **1**, $28.13(29)^{\circ}$ **2**). In addition, intramolecular CH···π contacts are found for **1** and **2** (Fig. S29, ESI[†]).

We performed cyclic voltammetry (CV) studies with **1** and **2** to study their redox properties (Fig. S21–S24, ESI[†]). Two oxidation events were observed for **1**, with a pseudo-reversible first one ($E_{1/2}(\text{Fc}^{0/+1}) = -0.1\text{ V}$) as indicated by the peak-to-peak distance ΔE_p value, which increased significantly with faster scan rates, followed by an irreversible second event ($E_{p,a}(\text{Fc}^{0/+1}) = 0.74\text{ V}$). In contrast, only one irreversible oxidation event was observed for **2** ($E_{p,a}(\text{Fc}^{0/+1}) = 0.66\text{ V}$), which occurred at a slightly lower voltage than the irreversible event of **1**. The reduction event found at $E_{p,c} = -0.79\text{ V}$ was observed only when the sample was scanned in the oxidative direction. The CV studies indicate that **1** can be oxidised by a mild oxidant, and **1** was therefore reacted with [Fc][BarF].¹⁹ The reaction immediately resulted in a color change (Scheme 2), and green crystals were isolated after workup, which did not show any paramagnetic behaviour. They were identified as [(Trip₂Sb)(TripSb)Naph][BarF] (**3**) and TripH was formed as a by-product. Analogous reactions in thf or CH₂Cl₂, which are easier to deprotonate than benzene, proceeded much faster, hence we assume that the Trip anion is protonated by the solvent. The splitted signals for the Naph protons in the ¹H NMR spectrum of **3** indicate an unsymmetric species. In addition, both sharp and broad signals in a 2:1 ratio are observed for the Trip protons. VT ¹H NMR studies showed a coalescence temperature of $-70\text{ }^{\circ}\text{C}$ for the sharp signals. The calculated rotational barrier ($\Delta G^{\ddagger} = 10.1\text{ kcal mol}^{-1}$) is roughly 5 kcal mol⁻¹ smaller than that in **1**, which is in line with the reduced steric hindrance due to removal of one Trip ligand. Comparable oxidation reactions were performed with **2**. Due to the higher oxidation potential, [NO][SbF₆] was chosen as the oxidant. The resulting reaction mixture showed high activity toward the polymerization of thf, but unfortunately, any attempts to isolate a product failed.

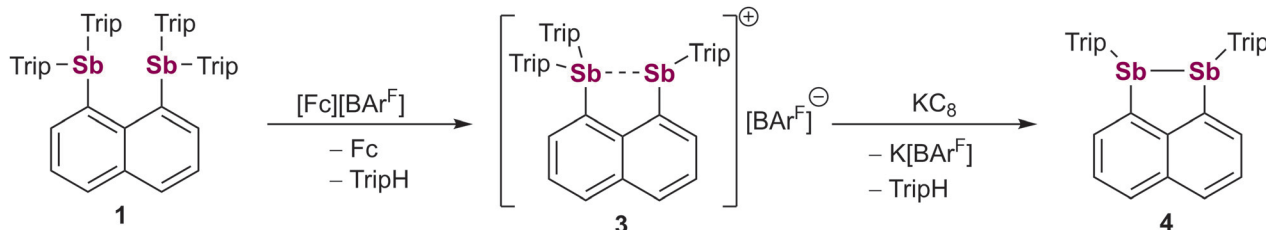
To transfer cation **3** into a radical species, we attempted a reduction with K₂C₈. A yellow solid was isolated after work-up and identified as (TripSb)₂Naph (**4**) (Scheme 2), while TripH and K[BarF] formed as by-products. The ¹H NMR spectrum of **4** shows the expected signals for a highly symmetric species.

Single crystals of **3** (Fig. 2B) and **4** (Fig. 2C) were grown from saturated solutions in 2 mL of CH₂Cl₂ layered with 30 mL of



Table 1 Selected bond lengths [Å] and angles [°] of **1–4**

1	2	3	4
Pn...Pn 3.2327(2)	3.6742(4)	2.7980(4)	2.7991(6)
Pn-C 2.1769(11), 2.2019(11), 2.1902(10)	2.318(4), 2.326(5), 2.326(5)	2.1170(15), 2.1367(15), 2.1465(15), 2.1647(17), 2.149(6), 2.196(6), 2.153(6), 2.192(6)	
C-Pn- 80.89(3), 93.23(3), Pn 167.59(3)	74.73(11), 102.87(13), 164.20(13)	91.26(4), 80.51(4), 137.25(4), 98.29(4), 106.31(4)	86.18(16), 100.81(17), 85.91(15), 102.91(15)
C-Pn-C 106.84(4), 101.51(4), 97.64(4)	107.53(16), 96.72(17), 92.31(9)	113.07(6), 113.33(6), 107.08(6), 102.86(6)	100.7(2), 99.9(2)

Scheme 2 Two-step reduction of **1** with elimination of TripH.

n-hexane (**3**) and in *n*-hexane (**4**) upon storage at +4 °C. **3** crystallises in the triclinic space group *P* $\bar{1}$ with two molecules per unit cell and **4** in the orthorhombic space group *Pbca* with eight molecules per unit cell. The Sb–C bonds in **3** and **4** are shorter than those in **1** as was expected, but the tetrahedrally-coordinated Sb1_1 atom in **3** (2.1170(5), 2.1367(15), 2.1465(15) Å) surprisingly shows slightly shorter Sb–C bonds than the three-coordinated Sb2_1 centers in **3** (2.1647(17), 2.1708(16) Å) and **4** (2.149(6), 2.196(6), 2.153(6), 2.192(6) Å), respectively. The Sb–Sb distance in **3** (2.7980(4) Å) is significantly shorter compared to that of **1** (3.2327(2) Å) and in the range of typical Sb(III)–Sb(III) bond lengths, indicating a strong Sb...Sb charge-transfer interaction. The Sb...Sb distance in **3** is virtually identical to the “regular” Sb–Sb single bond in **4** (2.7991(6) Å), and both are at the shorter end of the Sb–Sb bond length range reported for distibanes.²⁰

To interpret these experimental findings, quantum chemical computations were performed both for compounds **1–4** and the Ph-substituted reference systems **S1–S4** (see Fig. 3 and ESI†).

In the latter, the ligands at the Pn centers are not connected, so the Pn...Pn interactions can be determined by dividing the systems into two fragments. A comparison of the calculated data confirms that the Sb–Sb bond lengths in **3** (2.806 Å) and in **S3** (2.848 Å) are slightly shorter than that in **4** (2.820 Å) and in **S4** (2.860 Å), suggesting that the Sb–Sb binding in the cationic donor-acceptor compounds (**3**, **S3**) is stronger than in the distibanes (**4**, **S4**) containing a “regular” Sb–Sb covalent bond. Indeed, the total binding energy (ΔE in Fig. 3) obtained from a bond energy analysis calculation is higher for **S3** (Fig. 3, -64.2 kcal mol⁻¹) than for **S4** (-46.9 kcal mol⁻¹). A glance at the individual attractive energy terms for the Sb–Sb bonds in **S3** and **S4** reveals that they are very similar and quite different from the van der Waals interaction of the fragments in **S1** (Fig. 3). Thus, the relative sizes of the individual terms are not significantly different; in fact, in **S4** the electrostatic term is slightly larger than in **S3**; in other words, the dative Sb–Sb bond in **S3** is stronger than the covalent bond in **S4** due to orbital interactions. NBO analysis of **S3** and **S4** shows that the Sb–Sb bond in **S3** is strongly polarised (Fig. 3): the tetravalent Sb atom has a higher fraction (64%) and the *s* character of the orbital is significantly higher (22%) than that at the trivalent Sb atom (4%). As expected, a symmetric Sb–Sb bond with high *p* fraction (95%) of the interacting orbitals is found for **S4**. Quantum theory of atoms in molecules (QTAIM)²¹ analysis of **S3**, **S4**, **3** and **4** confirms these findings (Tables S10–S12 and Fig. S34–S39, ESI†). The Laplacian of the electron density ($\nabla^2\rho_{\text{BCP}}$) at the bond critical points (BCP) between the Sb atoms is in all cases negative which corresponds to polar covalent interactions. Furthermore, the BCPs in **S3** and **3** are closer to the tetravalent than to the trivalent Sb atom, indicating a polarised bond. A stabilising effect resulting from ligand–ligand dispersion interactions in **3/S3** relative to **4/S4** is negligible for the strength of the Sb–Sb bond.

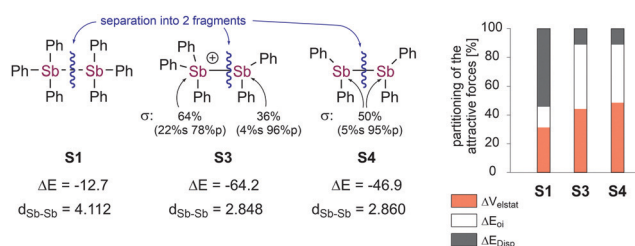


Fig. 3 Calculated (B3LYP-D3BJ/def2-TZVP) Sb...Sb distances [Å] in the reference systems **S1**, **S3** and **S4**. The percentage contributions of the attractive forces (ΔV_{elstat} , ΔE_{OI} and ΔE_{Disp}) and the total binding energies (ΔE in kcal mol⁻¹) between the Ph₂Sb fragments stem from bond energy analysis calculations (B3LYP-D3BJ/TZVP).



To conclude, stepwise single-electron oxidation and reduction reactions transformed the *peri*-substituted bisstibaphthalene (Trip₂Sb)₂Naph (**1**) via [(Trip₂Sb)(TripSb)Naph][BAR^F] (**3**) to the distibane (TripSb)₂Naph (**4**). A very strong donor-acceptor interaction is observed for the stibane-coordinated stibenium cation (**3-An**), resulting in a short Sb...Sb distance that is typical for regular Sb-Sb single bonds. According to quantum chemical calculations, the dative Sb-Sb bond in the related Ph-substituted system **S3** is stronger than the covalent Sb-Sb bond in **S4** due to orbital interactions.

Financial support by the DFG (SCHU1069/19-2) is acknowledged.

Conflicts of interest

There are no conflicts to declare.

Notes and references

- 1 G. C. Welch, R. R.-S. Juan, J. D. Masuda and D. W. Stephan, *Science*, 2006, **314**, 1124.
- 2 (a) D. W. Stephan, *Chem*, 2020, **6**, 1520; (b) J. Lam, K. M. Szkop, E. Mosafieri and D. W. Stephan, *Chem. Soc. Rev.*, 2019, **48**, 3592; (c) F. G. Fontaine and E. Rochette, *Acc. Chem. Res.*, 2018, **51**, 454; (d) W. Meng, X. Q. Feng and H. F. Du, *Acc. Chem. Res.*, 2018, **51**, 191; (e) D. W. Stephan, *Science*, 2016, **354**, 6317; (f) D. W. Stephan and G. Erker, *Angew. Chem., Int. Ed.*, 2015, **54**, 6400 (*Angew. Chem.*, 2015, **127**, 6498).
- 3 (a) M. Navarro, J. J. Moreno and J. Campos, *Frustrated Lewis Pair Systems, Reference Module in Chemistry, Molecular Sciences and Chemical Engineering*, 2022; (b) Q. Sun, C. G. Daniliuc, G. Kehr and G. Erker, *Dalton Trans.*, 2021, **50**, 3523; (c) B. J. Guddorf, A. Hepp, C. Daniliuc, D. W. Stephan and F. Lips, *Dalton Trans.*, 2020, **49**, 13386; (d) M.-A. Légaré, C. Pranckevicius and H. Braunschweig, *Chem. Rev.*, 2019, **119**, 8231; (e) Y. Ma, S. Zhang, C. R. Chang, Z. Q. Huang, J. C. Ho and Y. Q. Qu, *Chem. Soc. Rev.*, 2018, **47**, 5541; (f) J. Possart and W. Uhl, *Organometallics*, 2018, **37**, 1314.
- 4 (a) H. Steinert, J. Löffler and V. H. Gessner, *Eur. J. Inorg. Chem.*, 2021, 5004; (b) C. Mohapatra, L. T. Scharf, T. Scherpf, B. Mallick, K.-S. Feichtner, C. Schwarz and V. H. Gessner, *Angew. Chem., Int. Ed.*, 2019, **58**(22), 7459; (c) J. Schneider, C. P. Sindlinger, S. M. Freitag, H. Schubert and L. Wesemann, *Angew. Chem., Int. Ed.*, 2017, **56**, 333 (*Angew. Chem.*, 2017, **129**, 339); (d) J. Schneider, K. M. Krebs, S. Freitag, K. Eichele, H. Schubert and L. Wesemann, *Chem. – Eur. J.*, 2016, **22**, 9812; (e) S. Freitag, J. Henning, H. Schubert and L. Wesemann, *Angew. Chem., Int. Ed.*, 2013, **52**, 5640 (*Angew. Chem.*, 2013, **125**, 5750).
- 5 (a) M. Aman, L. Dostál, Z. Růžicková, S. Mebs, J. Beckmann and R. Jambor, *Organometallics*, 2019, **38**, 816; (b) M. Aman, Libor Dostál, T. Mikysek, Z. Růžicková, S. Mebs, J. Beckmann and R. Jambor, *Eur. J. Inorg. Chem.*, 2020, 3644.
- 6 J. M. Bayne and D. W. Stephan, *Chem. Soc. Rev.*, 2016, **45**, 765.
- 7 (a) Bi-P. Mokrai, J. Barrett, D. C. Apperley, A. S. Batsanov, Z. Benkő and D. Heift, *Chem. – Eur. J.*, 2019, **25**, 4017; (b) J. Burt, W. Levason and G. Reid, *Coord. Chem. Rev.*, 2014, **260**, 65.
- 8 J. L. Dutton and P. J. Ragogna, *Coord. Chem. Rev.*, 2011, **255**, 1414.
- 9 (a) A. P.-M. Robertson, P. A. Gray and N. Burford, *Angew. Chem., Int. Ed.*, 2014, **53**, 6050 (*Angew. Chem.*, 2014, **126**, 6162); (b) S. S. Chitnis, N. Burford, R. McDonald and M. J. Ferguson, *Inorg. Chem.*, 2014, **53**, 5359; (c) S. S. Chitnis, E. MacDonald, N. Burford, U. Werner-Zwanziger and R. McDonald, *Chem. Commun.*, 2012, **48**, 7359; (d) S. S. Chitnis, B. Peters, E. Conrad, N. Burford, R. McDonald and M. J. Ferguson, *Chem. Commun.*, 2011, **47**, 12331; (e) N. L. Kilah, S. Petrie, R. Stranger, J. W. Wielandt, A. C. Willis and S. B. Wild, *Organometallics*, 2007, **26**, 6106; (f) J. W. Wielandt, N. L. Kilah, A. C. Willis and S. B. Wild, *Chem. Commun.*, 2006, 3679.
- 10 (a) J. W. Wielandt, S. Petrie, N. L. Kilah, A. C. Willis, R. D. Dewhurst, F. Belaj, A. Orthaber, R. Stranger and S. B. Wild, *Aust. J. Chem.*, 2016, **69**, 524; (b) M. J. Ray, A. M.-Z. Slawin, M. Bühl and P. Kilian, *Organometallics*, 2013, **32**, 3481.
- 11 (a) J. Ramler, F. Fantuzzi, F. Geist, A. Hanft, H. Braunschweig, B. Engels and C. Lichtenberg, *Angew. Chem., Int. Ed.*, 2021, **60**, 24388 (*Angew. Chem.*, 2021, **133**, 24592); (b) C. Hering, M. Lehmann, A. Schulz and A. Villinger, *Inorg. Chem.*, 2012, **51**, 8212; (c) E. Conrad, N. Burford, R. McDonald and M. J. Ferguson, *Chem. Commun.*, 2010, **46**, 4598; (d) E. Conrad, N. Burford, R. McDonald and M. J. Ferguson, *J. Am. Chem. Soc.*, 2009, **131**, 5066; (e) H. J. Breunig, M. Denker and E. Lork, *Angew. Chem., Int. Ed. Engl.*, 1996, **35**, 1005 (*Angew. Chem.*, 1996, **108**, 1081); (f) H. Althaus, H. J. Breunig and E. Lork, *Chem. Commun.*, 1999, 1971.
- 12 (a) B. A. Chalmers, D. M.-U. K. Somisara, B. A. Surgenor, K. S. Athukorala Arachchige, J. D. Woollins, M. Bühl, A. M.-Z. Slawin and P. Kilian, *Molecules*, 2021, **26**, 7222; (b) B. A. Chalmers, M. Bühl, K. S. Athukorala Arachchige, A. M.-Z. Slawin and P. Kilian, *J. Am. Chem. Soc.*, 2014, **136**, 6247; (c) P. Kilian, F. R. Knight and J. D. Woollins, *Coord. Chem. Rev.*, 2011, **255**, 1387.
- 13 (a) P. S. Nejman, T. E. Curzon, M. Bühl, D. McKay, J. D. Woollins, S. E. Ashbrook, D. B. Cordes, A. M.-Z. Slawin and P. Kilian, *Inorg. Chem.*, 2020, **59**, 5616; (b) B. A. Chalmers, C. B.-E. Meigh, P. S. Nejman, M. Bühl, T. Lebl, J. D. Woollins, A. M.-Z. Slawin and P. Kilian, *Inorg. Chem.*, 2016, **55**, 7117; (c) B. A. Chalmers, M. Bühl, K. S. Athukorala Arachchige, A. M.-Z. Slawin and P. Kilian, *Chem. – Eur. J.*, 2015, **21**, 7520.
- 14 (a) C. Ganesamoorthy, S. Heimann, S. Hölscher, R. Haack, C. Wölper, G. Jansen and S. Schulz, *Dalton Trans.*, 2017, **46**, 9227; (b) K. Dzialkowski, A. Gehlhaar, C. Wölper, A. A. Auer and S. Schulz, *Organometallics*, 2019, **38**, 2927; (c) A. Gehlhaar, E. Schiavo, C. Wölper, Y. Schulte, A. A. Auer and S. Schulz, *Dalton Trans.*, 2022, **51**, 5016.
- 15 A. Gehlhaar, C. Wölper, F. van der Vicht, G. Jansen and S. Schulz, *Eur. J. Inorg. Chem.*, 2022, e202100883.
- 16 (a) J. Krüger, J. Haak, C. Wölper, G. E. Cutsail III, G. Haberhauer and S. Schulz, *Inorg. Chem.*, 2022, **61**, 5878; (b) H. M. Weinert, C. Wölper, J. Haak, G. E. Cutsail III and S. Schulz, *Chem. Sci.*, 2021, **12**, 14024; (c) C. Helling, G. E. Cutsail III, H. Weinert, C. Wölper and S. Schulz, *Angew. Chem., Int. Ed.*, 2020, **59**, 7561 (*Angew. Chem.*, 2020, **132**, 7631); (d) C. Helling, C. Wölper, G. E. Cutsail III, G. Haberhauer and S. Schulz, *Chem. – Eur. J.*, 2020, **26**, 13390; (e) J. Krüger, C. Wölper and S. Schulz, *Inorg. Chem.*, 2020, **59**, 11142; (f) C. Helling and S. Schulz, *Eur. J. Inorg. Chem.*, 2020, **3209**; (g) C. Helling, C. Wölper, Y. Schulte, G. Cutsail III and S. Schulz, *Inorg. Chem.*, 2019, **58**, 10323; (h) C. Ganesamoorthy, C. Helling, C. Wölper, W. Frank, E. Bill, G. E. Cutsail III and S. Schulz, *Nat. Commun.*, 2018, **9**, 87.
- 17 S. Sasaki, K. Sutoh, F. Murakami and M. Yoshifuji, *J. Am. Chem. Soc.*, 2002, **124**, 14830.
- 18 D. Kost, E. H. Carlson and M. Raban, *J. Chem. Soc. D*, 1971, 656.
- 19 N. G. Connelly and W. E. Geiger, *Chem. Rev.*, 1996, **96**, 877.
- 20 The Sb-Sb bond length in the complex [(CO)₄Cr(Sb₂Et₄)]₂ reported by Breunig et al. is significantly below any reported distibane to date. However, the authors present a highly disordered structure and can not exclude the presence of a second species. Therefore, the values should be treated with caution: H. J. Breunig, E. Lork, O. Moldovan and C. I. Raț, *Z. Naturforsch., B: J. Chem. Sci.*, 2013, **68**, 87.
- 21 R. F.-W. Bader, *Atoms in Molecules: A Quantum Theory*, Oxford University Press, Oxford, UK, 1990.

